Yang *et al. Zoonoses* (2024) 4:5
DOI 10.15212/ZOONOSES-2023-0049

ORIGINAL ARTICLE

Comparative Analysis of *Schistosoma japonicum* from Pairing-to-Sexual Maturation based on iTRAQ Proteomics

Wen-Bin Yang[1,#], Fang Luo[2,3,#], Rui-Xiang Zhang[2,3], Wei Zhang[2,3], Cheng-Song Sun[4], Qi-Mu-Ge Wu-Yun[1], Jing-Wei Quan[1], Yang Luo[1] and Wei Hu[1,2,3,*]

Abstract

Objective: Schistosomiasis, which is caused by the schistosome worm, poses significant health challenges. Understanding the sexual development and maturation of schistosomes would provide valuable insight for preventing the transmission of schistosomiasis and pathologic damage to the host.

Methods: Isobaric tags for relative and absolute quantitation (iTRAQ)-based proteomics was performed to monitor the dynamic proteomic profiles in *Schistosoma japonicum* during development from pairing-to-maturation. RNA interference (RNAi) experiments were used to elucidate sex-biased gene function.

Results: Of the 2927 identified proteins, 58.6% showed differential expression after comparing sexes and developmental stages. Both male and female worms displayed a similar number of gender-differentially expressed proteins after pairing. However, these proteins exhibited significant gender-specific functions, with reproduction central in females, while males were enriched in metabolic processes. Females exhibited 73% of their time-variant protein expression during 22-26 days post-infection (dpi), while males had 62% during 18-22 dpi, indicating earlier maturation in males. Functional analysis revealed different peptidases expressed during male and female development and maturation. Sex-biased *Sj*U2AF exhaustion led to worm development delay, abnormal reproductive organ development, and death.

Conclusion: Comparative proteomics enhances our understanding of mechanisms underlying schistosome maturation and reveals a new potential target for chemotherapy and vaccines.

Key words: *Schistosoma japonicum*, iTRAQ, proteomics, pairing, *Sj*U2AF

[#]These authors have contributed equally to this work.
***Corresponding author:**
E-mail: Huw@fudan.edu.cn (WH)

[1]The State Key Laboratory of Reproductive Regulation and Breeding of Grassland Livestock, School of Life Sciences, Inner Mongolia University, Hohhot, China
[2]State Key Laboratory of Genetic Engineering, Ministry of Education Key Laboratory of Contemporary Anthropology, Human Phenome Institute, Fudan University, Shanghai, China
[3]Ministry of Education Key Laboratory for Biodiversity Science and Ecological Engineering, Department of Microbiology and Microbial Engineering, School of Life Sciences, Fudan University, Shanghai, China
[4]Central laboratory, Anhui Provincial Institute of Parasitic Diseases, Anhui, China

Received: October 31 2023
Revised: December 6 2023
Accepted: December 20 2023
Published Online: January 6 2024

INTRODUCTION

Schistosomiasis is a parasitic disease caused by schistosomes. The World Health Organization (WHO) reported that this debilitating disease affected approximately 230 million individuals in 20189, predominantly in Africa, with > 50 countries requiring preventive therapy [1,2]. Three main schistosome species (*Schistosoma haematobium*, *S. japonicum*, and *S. mansoni*) infect humans and cause urogenital and intestinal schistosomiasis [3]. Schistosomiasis is classified as the most deadly neglected tropical disease (NTD) and the second most destructive

parasitic disease after malaria [4]. Schistosomes have a complex life cycle that spans seven distinct stages, alternating between sexual and asexual reproduction within two different hosts. Eggs hatch upon contact with water, releasing miracidia that penetrate specific snail intermediate hosts. Miracidia develop into sporocysts within the snails, which then produce daughter sporocysts through asexual reproduction, eventually giving rise to cercariae. The cercariae are released into the water and penetrate the skin of human hosts. After infection, cercariae transform into schistosomula and migrate through several tissues, eventually reaching the mesenteric veins. Schistosomula undergo pairing and mature into adult worms withing the mesenteric veins [5]. The final maturation in female worms depends on paring with males [6]. Most of the eggs laid by the adult worms induce hepatic granulomas; however, some of the eggs leave the body to hatch in water, which initiates a life cycle again [7,8].

Proteomic analysis has significantly enhanced our understanding of the molecular mechanisms pertinent to schistosome biology, encompassing various lifecycle stages and key biological components. This extensive analysis spans stages, such as eggs [9] and miracidium [10], as well as studies on vital biological materials, including cercarial secretions [11,12], extracellular vesicles, and schistosomula and adult worm tegument [13-17]. Comparative proteomic analysis has demonstrated that adult worms synthesize the proteins essential for gene expression and protein metabolism processes, while schistosomula proteins are mainly involved in the stress response pathway [16]. Notable differences in protein expression between male and female worms have been identified post-pairing, with these differentially expressed proteins largely associated with signal transduction, metabolism, immunity, and development [17]. Nevertheless, our grasp of the proteomic shifts from paring-to-maturation remains incomplete.

To elucidate proteomic changes throughout the development of *S. japonicum*, we utilized isobaric tags for relative and absolute quantitation (iTRAQ) to determine protein expression in male and female worms at various post-infection stages (14, 18, 22, and 26 days post-infection [dpi]). These time points represent pre-pairing (14 dpi), during pairing (18 and 22 dpi), and post-pairing (26 dpi) stages of schistosomes. Additionally, we used the RNA interference (RNAi) method to confirm that the development and reproduction of female worms likely involves activated or maintained proteins. Our findings revealed that *Sj*U2AF, a component of the consistently upregulated expression genes in female worms from 14–26 days, is essential for maintaining normal worm growth and reproduction. Notably, exhaustion of *Sj*U2AF resulted in significant *S. japonicum* developmental delay or mortality. This research is poised to enrich our understanding of the maturation mechanism underlying *S. japonicum* and accelerate the creation of new therapeutic strategies against this critical, yet NTD.

MATERIALS AND METHODS

Ethical statement

All animal experiments were approved by the Ethics Committee of the National Institute of Parasitic Diseases of the Chinese Center for Disease Control and Prevention in Shanghai, China (reference no.: IPD-2020-10).

Animals and parasites

Oncomelania hupensis snails were provided by the Department of Vector Control of the National Institute of Parasitic Diseases. Cercariae (Anhui isolate) were released from *S. japonicum*-infected snails. Six-week-old female C57BL/6 mice were purchased from the Shanghai Animal Center (Chinese Academy of Sciences, Shanghai, China). Each mouse was infected with 60 ± 5 cercariae. We organized the mice into 12 groups, corresponding to four time points (14, 18, 22, and 26 dpi) in triplicate at each time point. Schistosomes were harvested from mice at the four time points through hepatic-portal perfusion. Subsequently, female and male schistosomes were manually separated under light microscopy.

Protein preparation and iTRAQ labeling

Protein extraction was carried out using the filter-aided sample preparation method [18]. The female and male schistosomes collected at each time point were resuspended in SDT buffer (4% SDS, 30 mM triethylammonium bicarbonate [TEAB], and 2 mM DTT) at 95 °C for 5 min, followed by brief sonication. Prior to protein extraction, the lysate was centrifuged at 14,000 g for 20 min at 20 °C. The protein concentration in each supernatant was quantified using a Pierce BCA Protein Assay Kit (Thermo Fisher Scientific, Waltham, MA, USA). Subsequently, 200 μg of each lysate supernatant was mixed with 200 μl of extract buffer (7 M urea, 2 M thiourea, and 30 mM TEAB). This mixture was placed in an ultrafiltration unit (10 K; Millipore, Billerica, MA, USA) and centrifuged at 14,000 g for 40 min. The flow-through was discarded after each centrifugation and the process was repeated 3 times with fresh extraction buffer. A standard procedure recommended by the manufacturer's instructions was followed for iTRAQ labeling. Briefly, each protein sample was reduced, alkylated, and digested with trypsin (Promega, Madison, WI, USA). The digested peptides were then dried and labeled using the iTRAQ Reagents-8plex (Thermo Fisher Scientific, Waltham, MA, USA). After labeling, the samples were mixed together and prepared for mass spectrometry analysis.

HPLC-MS/MS analysis

High pH high-performance liquid chromatography (HPLC) was performed using a BioBasic SCX column (2.1 [internal diameter] × 150 mm [length]; Thermo Fisher Scientific, Waltham, MA, USA) with a particle size of 5 μm and a pore size of 300 Å. The mobile phase was comprised of buffer A (10 mM ammonium acetate [pH = 10.0]) and buffer B (10 mM ammonium acetate and 80%

acetonitrile {ACN} [pH = 10.0]). The column was initially washed with buffer A at a flow rate of 200 μl/min for 10 min, followed by a gradient elution from 0% to 50% (buffer B) in buffer A at 200 μl/min for 15 min. The next phase involved a 5-min gradient from 50% to 100% (buffer B) in buffer A at 200 μl/min, returning to 0% (buffer B) in 5 min at 350 μl/min, and concluding with a final wash for 15 min in buffer A at 350 μl/min. The sample loading size was 87 μg. Eluent fractions were collected every minute, lyophilized, and stored at −20 °C for later use.

Liquid chromatography-tandem mass spectrometry (LC-MS/MS) was performed on an EASY-nLC 1000 system coupled to an LTQ-Orbitrap mass spectrometer (Thermo Fisher Scientific, Bremen, Germany). Before ionization, the samples flowed through a guard column (Acclaim PepMap100 C18 Nano Trap column [5 μm, 100 Å, 100 μm {internal diameter} × 2 cm {length}]; Thermo Fisher Scientific, Sunnyvale, CA, USA) and an analytical column (Acclaim PepMap RSLC C18 column [2 μm, 100 Å, 75 μm {internal diameter} × 25 cm {length}]; Thermo Fisher Scientific, Sunnyvale, CA, USA). Briefly, lyophilized samples were dissolved in 1% trifluoroacetic acid (TFA) before application onto the column equilibrated in a mobile phase consisting of buffer A (0.1% formic acid [FA]). The elution gradient in buffer A of buffer B (0.1% FA, 100% ACN) over 2 min was from 2% to 5%, followed by gradient steps: 2-100 min in buffer B from 5% to 28%; 100-105 min in buffer B from 28% to 35%; 105-107 min in buffer B from 35% to 90%; and a final wash from 107-120 min in 90% buffer B. We used data-dependent acquisition and the top 15 precursor peaks were selected for MS^2 with a higher energy collisional dissociation (HCD).

The raw MS data were analyzed using Proteome Discoverer software (version 1.4; Thermo Fisher Scientific, Waltham, CA, USA) in conjunction with an in-house Mascot server (version 2.3; Matrix Science, London, U.K.) against the *S. japonicum* V 4.0 protein database (http://schistoDB.net/). Analytical parameters were set as follows: trypsin was selected as the digestion enzyme; maximum missed cleavage sites were set at 2; precursor and fragment mass tolerance were set to 10 ppm and 0.05 Da; carbamidomethyl (C), iTRAQ 8plex (K), and iTRAQ 8plex (N-term) were used as static modifications; and oxidation of methionine was used as the variable modification. The resulting peptide and protein data were organized in S1 Table. The mass spectrometry proteomics raw data have been deposited in the iProX database under the identifier, IPX0001042002.

Experimental Design and Statistical Rationale

To enhance reliability in protein identification, we utilized the Target Decoy PSM Validator in Proteome Discoverer, setting a stringent false discovery rate (FDR) threshold of ≤ 0.01. Proteins identified with a minimum of one unique peptide were considered credible. The experiment contained three biological replicates for each of eight samples distributed across three independent eight-plex iTRAQ experiments. iTRAQ quantitative data are presented as the individual report ion intensity-to-total report ion intensity ratio. Quantitative comparisons were calculated with central tendency normalized protein values. Statistical analysis was performed using Student's t-test to compare biological replicates. Proteins with a p-value < 0.05 and a fold-change > 1.5 or < 0.66 were classified as differentially expressed. Principal component analysis (PCA) analysis and hierarchical clustering were performed using OmicShare tools, a free online platform for data analysis (http://www.omicshare.com/tools) with default parameters. Gene ontology (GO) enrichment analysis was performed to pinpoint specific biological functions enriched among the identified and differentially expressed proteins. The metabolic pathways involved were constructed using the Kyoto Encyclopedia of Genes and Genomes (KEGG) Automatic Annotation Server (http://www.genome.jp/tools/kaas/) with the single-directional best-hit assignment method. Annotated peptidases were analyzed using MEROPS (release 11.0; https://www.ebi.ac.uk/merops/) for gene family identification.

Molecular function of the *S. japonicum* target journal

RNA whole mount *in situ* hybridization (WISH) experiment was performed to elucidate target gene function. The worms were fixed with 4% paraformaldehyde dissolved in PBSTX (1X PBS and 0.3% TritonX-100). A target-specific riboprobe was designed using primers software to detect the target transcripts (S6 Table). The WISH procedure was performed as previously described and the targeting sequence location was examined microscopically using a Nikon 80i microscope (Nikon Corp., Tokyo, Japan).

For dsRNA interference, the *Sj*U2AF dsRNA sequence was synthesized with the MEGAscript T7 transcription kit (Thermo Fisher Scientific, Waltham, MA, USA). A non-specific dsGFP RNA sequence served as the negative control. Six freshly perfused pairs of worms were exposed to 20 μg/ml of dsRNA in 3 ml of medium in a 12-well plate (DMEM, 10% fetal bovine serum, 1% HEPES buffer, and 2% penicillin/streptomycin solution) for *in vitro* RNAi experiments. The worms were monitored daily for motility and viability for up to 30 days, with the culture refreshed every other day [19,20]. Each mouse was infected with 60 ± 3 cercariae and immediately injected with 10 μg (25 pmol) of dsRNA dissolved in 0.2 ml of saline buffer (0.7% NaCl) via the tail vein for *in vivo* RNAi experiments, followed by repeated injections every 4 days. The schistosomula were exposed to the dsRNA for 30 days, then collected as previously described [21]. The harvested worms were divided into two groups for further analysis. One group was fixed in alcohol-formalin-acetic acid (AFA) and stained with carmine red; the other group was fixed in 75% alcohol and stained with Fast Blue B. Both groups were then imaged by light microscopy

(Nikon 80i) and confocal laser scanning microscopy ([CLSM] Nikon A1-Ni; Nikon Corp., Tokyo, Japan).

RESULTS

Male and female worms developed at different rates from pairing-to-maturation

We identified 27538, 23116, and 22360 peptides across 3 replicates. A total of 4666 protein groups were detected in at least 1 replicate, covering 37% of the predicted *S. japonicum* proteome in the *Sj*_V 4.0 database (accession number: ASM15177v1). Notably, 81.0% (3779/4666) of these protein groups were identified in at least 2 of the 3 replicates (Fig 1A). For further comparative analysis, we specifically focused on a subset of 2927 proteins identified with 8 iTRAQ labels across all replicates (S2 Table). The consistency in values across all three replicates for each time point without any outliers underscored the robustness and high quality of the data obtained in this study. GO enrichment analysis showed that 88.0% of the

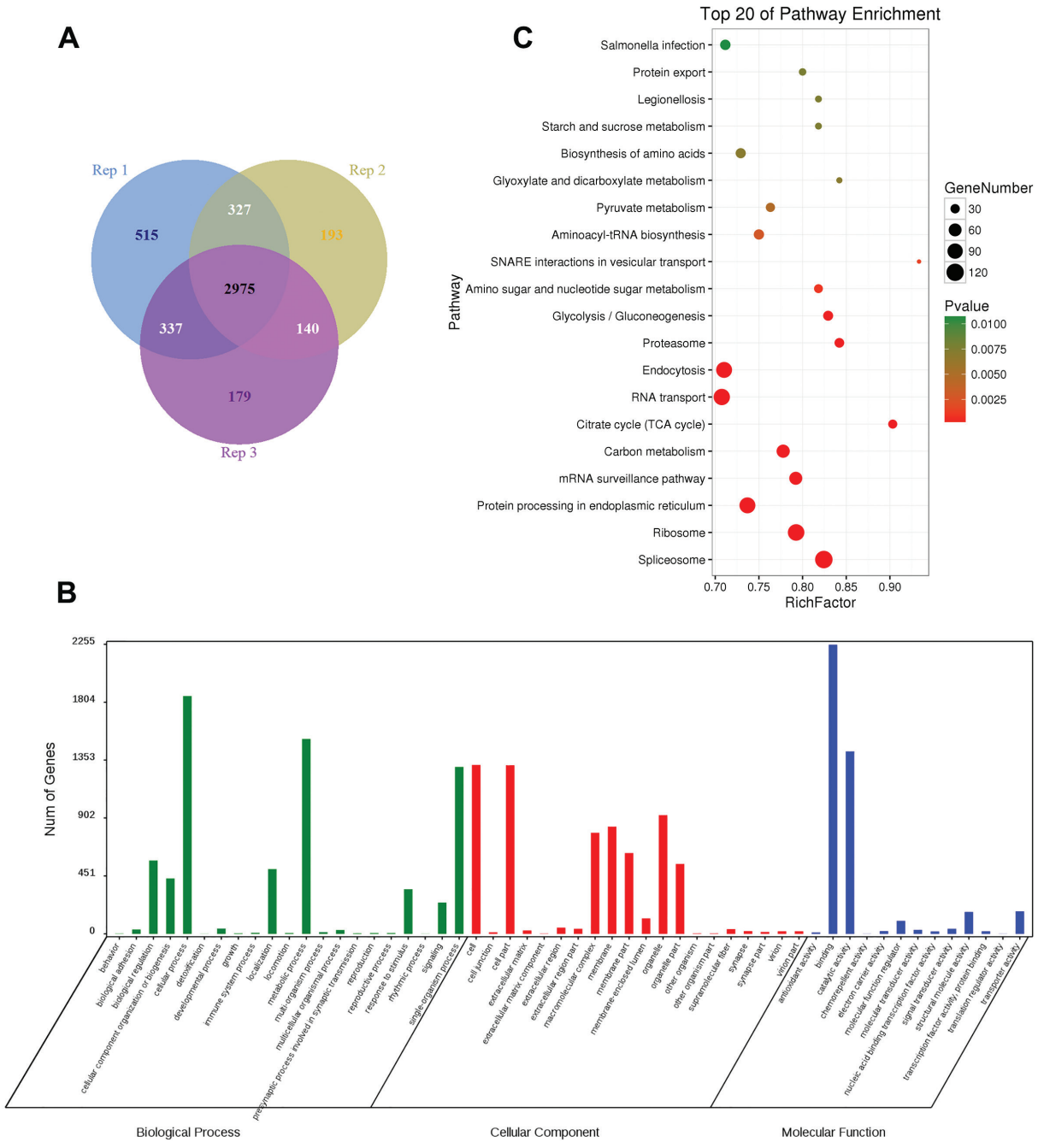

FIGURE 1 | Global view of identified proteins. (A) Venn diagrams of identified proteins, including three biological replicates. (B) Gene ontology (GO) annotation of total identified proteins. The chart describes the GO distribution of GO terms on level 2. (C) KEGG analysis of identified proteins showing the top 20 enriched KEGG pathways.

identified proteins were classified into 54 distinct GO categories. The 4 most prevalent categories, which comprised 48.3%, 39.7%, 32.5%, and 30% of all identified proteins, were categorized as binding, cellular processes, metabolic processes, and catalytic activity respectively (Fig 1B). KEGG pathway analysis further revealed that these identified proteins were involved in 311 distinct pathways, which could be grouped into 6 classes. Among these pathways, the most significantly enriched pathways during schistosome development were related to "carbohydrate metabolism," "translation," and "folding, sorting, and degradation" (Fig 1C). SNARE interactions in vesicular transport, the TCA cycle, and proteasome pathways were also highly enriched.

PCA analysis showed distinct protein expression distributions throughout the developmental period (S1 Fig). At 14 dpi, when the worms were in the schistosomula stage, males and females exhibited similar protein expression profiles. As development progressed, however, a noticeable divergence in protein expression between genders was observed beginning at 18 dpi. For females, the protein profiles at 18 and 22 dpi appeared similar, yet distinct from 26 dpi, indicating a later maturation. In contrast, male worms exhibited a near-mature protein expression profile between 22 and 26 dpi, diverging from the 18 dpi profile. Because the 16–22 dpi window was identified as the schistosome pairing period, worms were considered adults 26 dpi. This data pattern suggests differential developmental rates between male and female worms, with females requiring a longer period to reach maturity.

Of 2927 proteins, 1714 (58.6%) were identified as differentially expressed proteins (DEPs) after sex and developmental stage comparisons. Hierarchical cluster analysis of these DEPs revealed clear distinctions between male and female worms (Fig 2A). Immature males and females at 14 dpi were grouped together initially but separated at 18 dpi. The male worm DEPs at 18, 22, and 26 dpi were clustered together, whereas for females DEPs at 18 and 22 dpi were similar but distinct from 26 dpi. The DEPs were further grouped into three subclusters with distinct expression patterns across different sexes and developmental stages (Fig 2B). Proteins in cluster 1 were predominantly upregulated in male worms following pairing. GO enrichment analysis revealed that these proteins were associated with protein localization, catabolic processes, and carbohydrate metabolic processes. Conversely, proteins in cluster 2 were gradually upregulated in female worms following pairing. The DEPs in this cluster were enriched in functions related to protein folding, translation, and cellular component morphogenesis. Proteins in cluster 3 exhibited higher expression in the schistosomula stage for male and female worms. These proteins were mainly involved in macromolecule metabolic processes, chromatin remodeling, DNA replication initiation, and post-transcriptional regulation of gene expression (Fig 2C).

Evaluation of quantified protein expression profiles

To validate the robustness of our dataset, we examined the expression profiles of select individual proteins. We checked the expression profiles of housekeeping proteins, such as the proteasome 26S subunit (PSMD, Sjp_0007000), tubulin (tubulin gamma-1 chain, Sjp_0036720), and actin (actin subunit, Sjp_0005140). We observed a stable expression of these proteins across all *S. japonicum* samples, with no regulation differences

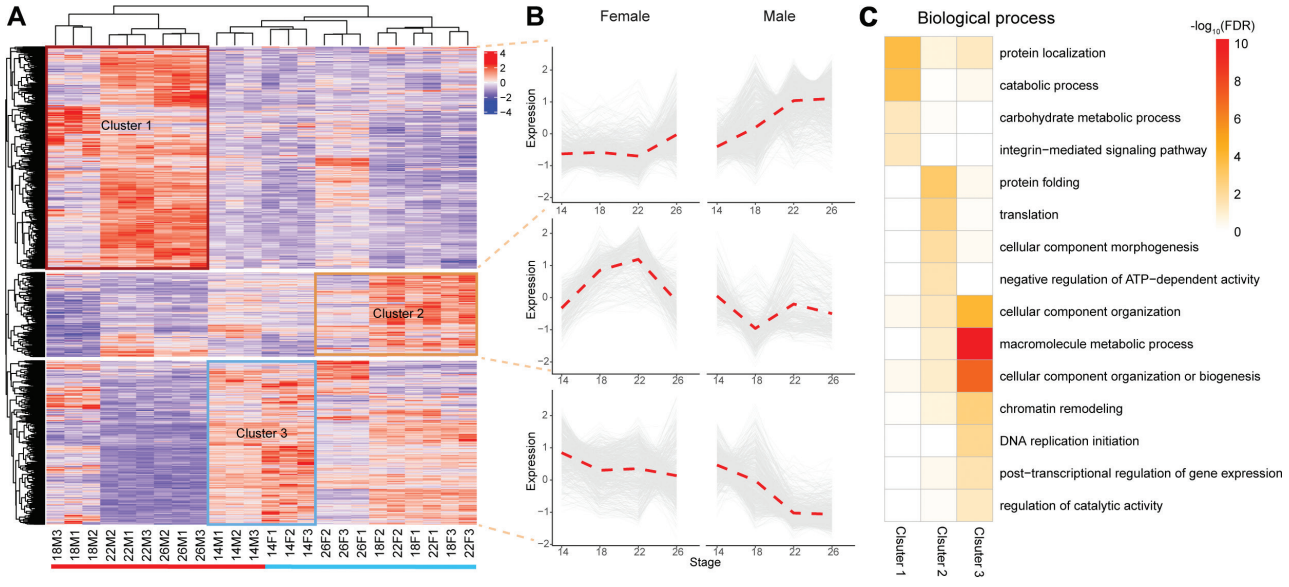

FIGURE 2 | Hierarchical clustering of the differentially expressed proteins (DEPs). (A) Heatmap plot of the 1714 DEPs using the hierarchical clustering method; three sub-clusters are shown (F: female, M: male). (B) Patterns of protein expression in three clusters for male and female worms corresponding to the hierarchical heatmap. Red lines show the average values for the relative expression levels in each sub-cluster. (C) GO enrichment analysis of the DEPs in three sub-clusters.

noted between gender or developmental stages (S2 Fig). A previous study showed that ferritin-1, which is responsible for iron transport, was predominantly detected in female worms [22] and upregulated at 23 dpi compared to 18 dpi worms [23]. Ferritin-1 (Sjp_0201280) was specifically and highly expressed in 26 dpi females. Additionally, we determined the patterns of the Rab family of proteins expression, known for their potential roles in tegument turnover. Previous studies have suggested elevated SmRab expression in male worms [24]. Our dataset revealed that several Ras-related proteins were highly expressed in male worms, particularly Rab-8 (Sjp_0044620) and Rab-3C (Sjp_0113630), which displayed a male-biased expression pattern from 22 dpi onwards. In summary, the assessment of these specific protein expression profiles reinforces the credibility of our data in depicting the development process of *S. japonicum*.

Significant difference between the levels of gender-specific protein expression occur during the last pairing phase

To understand the gender-biased protein functions during schistosome pairing and maturation, we performed a comparative analysis of protein expression between male and female worms at each time point (Fig 3A). From 14–26 dpi, noticeable differences in protein expression were observed between genders. At the initial stage of 14 dpi, gender differences were negligible, with only 49 proteins showing gender-biased expression. Upon pairing, however, DEPs between genders increased markedly and culminated at 22 dpi with up to 510 DEPs in females and 496 DEPs in males. The differential expression was then reduced slightly at 26 dpi.

Interestingly, despite a similar count of gender-biased proteins in each gender at 18 and 22 dpi, GO enrichment analysis revealed a considerable difference. At 18 dpi, the 263 female-biased proteins were significantly divided into 132 GO categories compared to only 16 categories in male-biased proteins (S2 Table). These DEPs were involved in various processes in females, with regulation, and complex and metabolic processes most predominant. These DEPs also participated in many pathways, particularly pathways related to signal transduction and translation (Fig 3C). These DEPs were significantly enriched in the GO terms related to cytoplasm, ribosome biogenesis, and benzoate and olefin metabolic processes in 18 dpi male worms (S2 Table).

As pairing proceeded, the impact on gender-biased protein function began to reverse at 22 dpi, with significant enrichment of 52 and 145 categories in female and male worms, respectively (S2 Table). Substantial enrichment in 64 metabolic processes was noted in male worms, particularly with respect to peptide and glucose metabolism. Additionally, eight biosynthetic processes and six oxidoreductase activity functions were also enriched. Conversely, DEP functions in females focused on translation and transcription processes (Fig 3D).

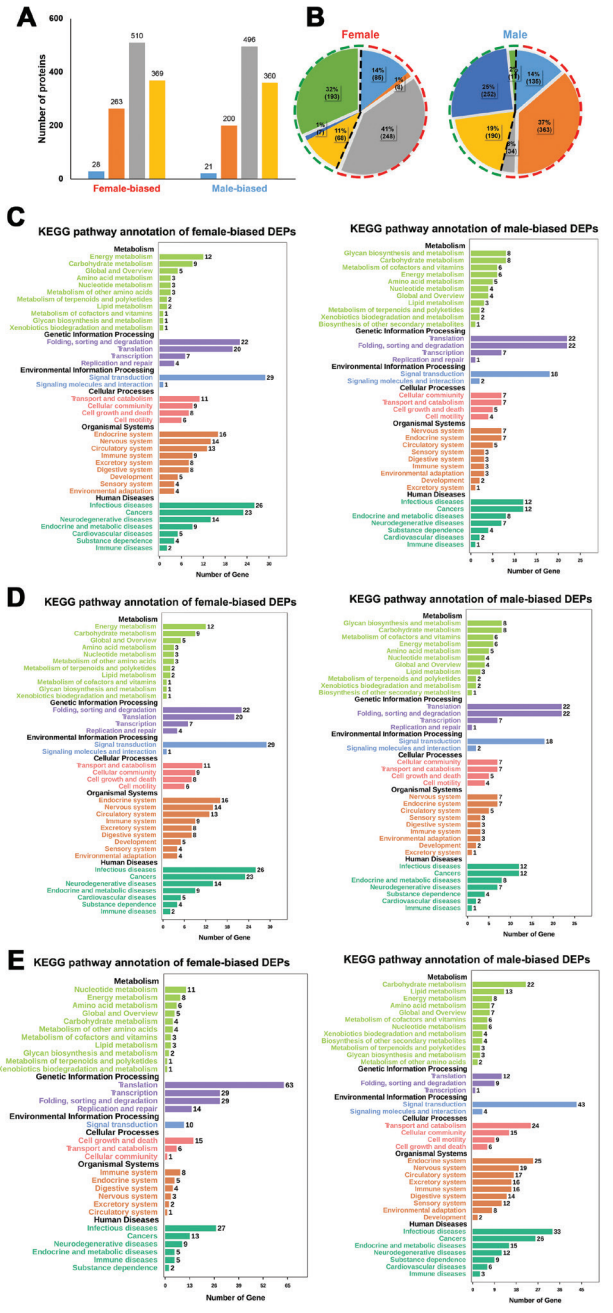

FIGURE 3 | Number of DEPs and annotations in KEGG pathways. (A) Sex-biased DEPs at each time point (blue: 14 dpi, orange: 18 dpi, grey: 22 dpi, yellow: 26 dpi). (B) Stage-regulated DEPs at adjacent time points. Upregulated: light blue (14-18 dpi), orange (18-22 dpi), and grey (22-26 dpi). Downregulated: yellow (14-18 dpi), blue (18-22 dpi), and green (22-26 dpi). Sex-biased DEPs involving KEGG pathway annotation of 18 dpi (C), 22 dpi (D), and 26 dpi (E) worms.

Adult male and female worms exhibited approximately 100 enriched GO categories each at 26 dpi after pairing (S2 Table). Biosynthetic and binding functions, including small molecule, nucleotide, and RNA binding, were abundant in females. Male worms displayed a dominance of metabolic and catabolic processes, particularly related to polysaccharides, glycogen, and glucan. KEGG annotation analysis at 26 dpi revealed that DEPs in male worms

participated in > 200 different pathways, while 16.1% (63/390) of DEPs in females were associated with the translation pathway (Fig 3E). The DEP mapped pathways were more diverse in males but more focused in females. Taken together, these findings indicated that adult schistosomes display a distinct sex-biased division in protein functions at 26 dpi.

Expression of proteins remains unchanged 18-22 dpi in female worms

To understand the dynamic changes in protein function over time in *S. japonicum*, we compared protein expression between adjacent time points for each gender. Many proteins were differentially expressed as development progressed. Interestingly, females and males displayed distinct patterns of protein expression changes (Fig 3B). In females, protein expression changed little from 18–22 dpi, with approximately 73% of the time-variant protein expression occurring during the 22-26 dpi period. However, in the early stages (14-18 dpi), both male and female worms exhibited similar expression trends.

In the early developmental phase (14–18 dpi) females showed altered 153 protein expression, with 85 proteins upregulated and 68 proteins downregulated. Proteins related to metabolic and single-organism processes were upregulated. In contrast, proteins involved in binding activities were downregulated (S3 Fig). Conversely, only 15 proteins (8 upregulated and 7 downregulated) exhibited altered expression between the 18 and 22 dpi in females. These changes could be caused by heterogeneity in female development because only 174 proteins fulfilled the *p*-value criteria (< 0.05) when comparing 18 and 22 dpi female worms.

As the ovary and vitelline glands begin to develop post-pairing, we observed significant variations in the expression of > 400 proteins between 22 and 26 dpi, with 248 proteins being upregulated and 193 downregulated. GO enrichment analysis of these proteins identified metabolic and cellular processes, as well as the activity of upregulated structural proteins (S4 Fig). Other biosynthetic-, translation-, and biogenesis-related processes were also significantly upregulated, while oxidoreductase activity was significantly downregulated (S2 Table).

Protein expression profile of male worms stabilized by 22 dpi

May expression profiles of proteins varied until 22 dpi in males. A total of 325 proteins showed alterations in expression (135 upregulated and 190 downregulated) from 14–18 dpi and 615 proteins were variably expressed (363 upregulated and 252 downregulated) from 18–22 dpi. Variability in expression profile was less pronounced after pairing, with only 51 proteins showing signs of regulation.

GO enrichment analysis showed that between 14 and 18 dpi, no specific biological process was significantly upregulated in males, while organelles and other processes were significantly downregulated (S2 Table and S5 Fig). KEGG annotation indicated that many metabolism pathways were upregulated between 14 and 18 dpi, including carbohydrate, glycan, amino acid, and energy metabolism. Downregulated pathways focused on translation and signal transduction (S7 Fig).

From 18–22 dpi, binding functions and cellular processes were the most abundantly regulated processes. Among the 363 upregulated proteins in males, 132 GO categories were significantly enriched, including 6 transmembrane activities and 6 oxidoreductase activities (S2 Table and S6 Fig). Many cellular processes were downregulated, but no biological processes or molecular functions were significantly enriched. Additionally, 37 signal transduction pathways and many metabolic pathways were upregulated (S8 Fig).

Using protein expression profiles as a guide, male schistosome worms were shown to nearly reach maturation at 22 dpi in the last phase of pairing. This finding is consistent with the upregulation of energy metabolism, binding functions, and various other activities that male worms developed since pairing and before maturation at 26 dpi.

Similarities and differences between dynamic proteomic and transcriptomic expression profiles

In our previous study we monitored the dynamic transcriptomic profiles of *S. japonicum* throughout sexual development [25]. Greater than 50% of identified transcripts in that study were also detected in our proteomic analysis (S10 Fig). The dynamic transcriptomic profiles suggested that gender-differentially expressed transcripts increased markedly at 22 dpi, mirroring the trends observed in this current proteomic study. A slight decrease in female-biased transcripts from 24–26 dpi was also observed in the protein expression profiles between 22 and 26 dpi in the present study. Furthermore, this correlation extended to the protein functional groups, with categories like ribosome, chromosome, oocyte maturation, translation, DNA repair, and metabolic processes, being enriched in both mRNA and protein levels in female worms. Dramatic changes were evident in females post-pairing in mRNA and protein expression profiles with respect to the temporal regulation, with 15.1% of proteins and 16.8% of transcripts showing alterations during the 22-26 dpi period.

The functional grouping of sex-biased expressed genes between transcriptomes and proteomes at the same developmental stages had a low correlation. Only a few proteins and their corresponding transcripts, whether male- or female-dominant, were consistent at the same developmental point. However, the number of proteins in which expression profiles were altered in a manner similar to the mRNA transcriptome profile increased in each gender from 18–26 dpi (S3 Table). Only 4.2% of the *de novo* transcripts were female-dominant at 26 dpi and 11.1% were male-dominant transcripts. At the same time, 12.6% (369/2927) of quantified proteins were female-biased and 12.3% (360/2927) were male-biased. It is notable that the overall number of female-biased genes at the four-time

points were less than male-biased genes at the transcript level, while most sex-biased genes were constant at the protein level.

Signaling pathways in male and female worms are displayed in different ways

By 22 dpi, male worms had nearly matured, while in female worms the development of ovaries and vitelline glands were just beginning. Hence, 22 dpi can be defined as a crucial time point in the development of both genders. To better understand the regulatory mechanisms post-pairing, we focused on the gender-biased DEPs-involved pathways at 22 and 26 dpi (S11 Fig). Altogether, 276 pathways were involved, 200 of which were shared between 22 and 26 dpi male worms, and 91 were shared between 22 and 26 dpi females. One hundred one pathways were regulated at 22 dpi but not at 26 dpi in female worms compared to only 46 pathways differing between 22 and 26 dpi in male worms. Of the 276 regulated pathways, 45 were shared in 22 and 26 dpi sex-biased DEPs, excluding those classified under "human diseases" (S4 Table).

According to KEGG pathway annotation analysis, the three most abundant processes were "translation," "signal transduction," and "folding, sorting, and degradation." This indicated that after pairing, male and female worms appeared to regulate the same pathways, primarily those required for fundamental biological processes, although this occurred through different proteins. These pathways mainly included the mRNA surveillance pathway, spliceosomes, RNA transport, the mRNA surveillance pathway, protein processing in the endoplasmic reticulum, ribosomes, and endocytosis. In addition, other pathways have been identified and characterized, such as the Notch, Wnt signaling, Bcl-2-regulated apoptosis, MAPK, and histamine signaling pathways. These pathways might be essential for the pairing-dependent differentiation of the reproductive organs.

Males and females had similar protein expression profiles at 14 dpi in *Schistosoma*. The number of sex-differentiated proteins increased 18 dpi after pairing. The mechanisms involved in controlling the growth and sex differentiation processes of schistosomes at specific time points has not been established. Based on studies involving the evolutionarily-conserved signaling pathway spliceosomes in other species, spliceosomes may also play a key role in regulating the reproductive and developmental processes of *Schistosoma*. Moreover, during trend clustering protein functional analysis, we showed that U2 small nuclear RNA auxiliary factor 2 (U2AF, Sjp_030142) was consistently upregulated in females, suggesting a potential association with female growth or reproductive organ development.

Morphometry and Morphology of U2AF-silenced parasite

To explore our hypothesis regarding roles of *Sj*U2AF in *S. japonicum*, in situ hybridization was performed. Transcriptional signals of *Sj*U2AF were observed in the tegument, stem cells, and reproductive organs of both male and female worms (Fig 4A), implying its importance in growth and reproductive system development. To further understand the function of *Sj*U2AF, we knocked down the target gene using RNAi technology in *S. japonicum*. *In vitro* worm culture experiments showed a significant reduction in *Sj*U2AF expression after 8 days of dsRNA treatment (Fig 4B), resulting in impaired adherence of parasites to cell culture surfaces and a notable disruption in pairing between male and female worms. A majority of worms turned black with > 80% mortality after 14 days (Fig 4C). We further determined whether knockdown *Sj*U2AF affected worm growth and development in the mouse model. Interestingly, exhaustion of *Sj*U2AF led to significant worm mortality *in vivo* compared to the control with significant growth and development impairment (Fig 4D and E). These results further confirmed that *Sj*U2AF has a pivotal role in the survival and development of *S. japonicum*.

In addition, we investigated the development of reproductive organs in surviving worms. Fast Blue B staining showed that female worms failed to develop mature vitellarium and showed less pigmentation in intestinal tissues (Fig 4F). Laser scanning confocal microscopy images showed underdeveloped oocytes and disorganized vitellarium in females, and immature spermatocytes in male testes (Fig 4G). Additionally, fewer granulomas were present in the livers of mice in the RNAi-U2AF group during the acquisition of worms, suggesting reduced egg production (Fig 4H). These results conclusively demonstrated that knockdown of *Sj*U2AF severely impacts the development of reproductive organs in *S. japonicum*, affirming a significant role in parasite reproductive and developmental processes.

DISCUSSION

Liu *et al*. [26] first characterized the expression profiles of genes and proteins across the different developmental stages of *S. japonicum*. The transcriptome data showed that sex-enriched expression was far more dramatic than stage-enriched expression, a finding that aligns with our quantitative proteomics data (1450 sex-biased DEPs and 1180 stage-biased DEPs). Since then, proteomic studies involving schistosomes have made remarkable progress, including investigations into tegument proteins [27-29], the soluble proteome [30], the excretory/secretory proteome [31], and post-translational modification proteomics [32-34]. These studies have illuminated the multifaceted roles proteins play in the lifecycle of worms, encompassing development, the host-parasite interaction, and sex- and immune-related processes.

Our study tracked the dynamic changes in relative protein expression during the development of *S. japonicum* from pairing-to-maturation. The present study used an iTRAQ-based proteomics method to identify DEPs

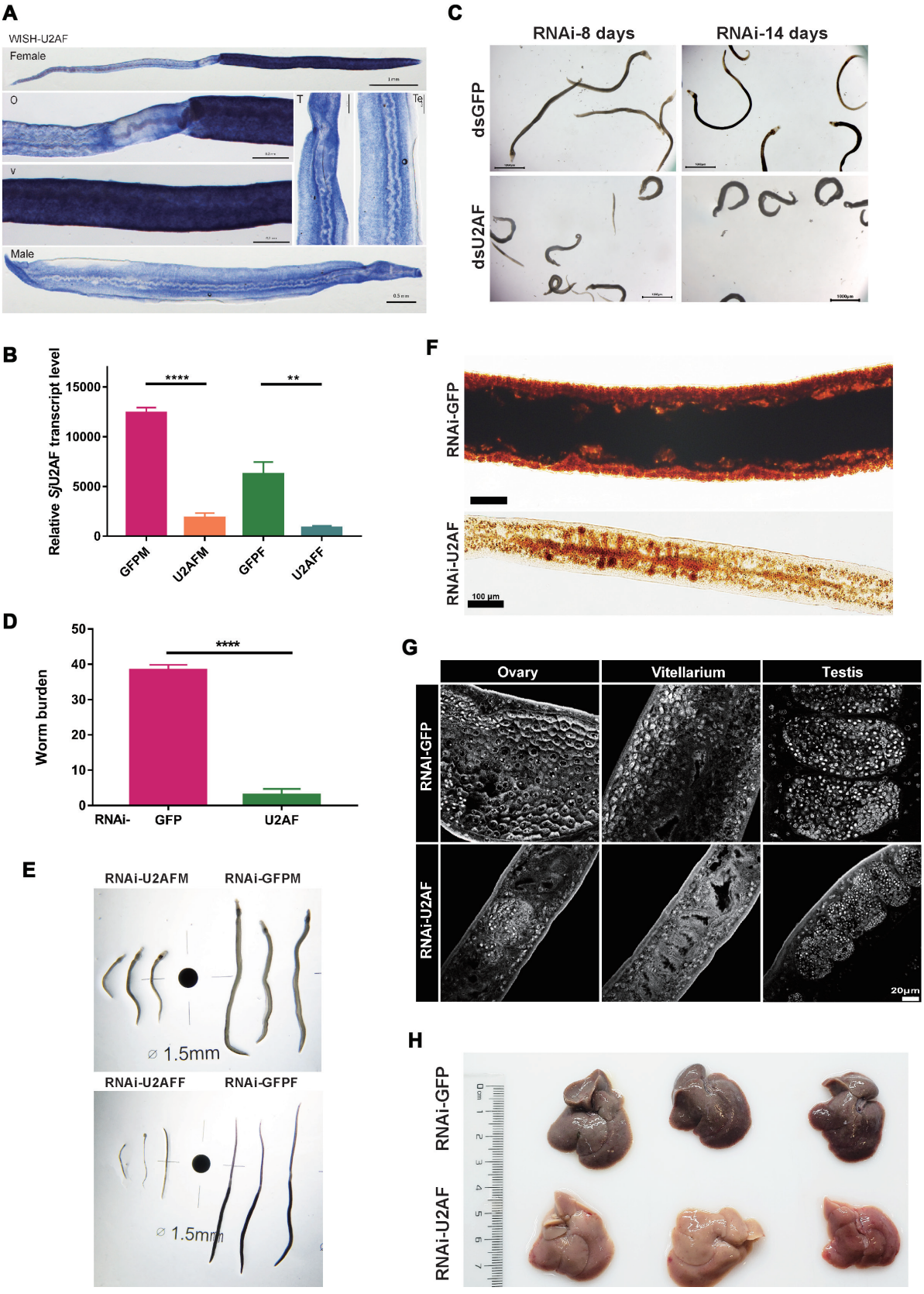

FIGURE 4 | Effect on the viability and development of *S. japonicum* after *Sj*U2AF knockdown. (A) *In situ* hybridization analysis of *Sj*U2AF in worms. (B) Efficacy assessment of dsRNA-mediated *Sj*U2AF knockdown. All experiments were performed in triplicate with three biological replicates. (C) Effects on worm motility of dsU2AF treatment. (D) The number of worms collected 30 dpi from dsRNA-injected mice. Each group had three biological replicates. (E) Comparison of the length of male and female worms. (F) Microscopy images of Fast Blue B-stained female worms. (G) Confocal laser scanning micrographs documenting morphologic changes in the reproductive organs of *S. japonicum*. (H) Comparative images of liver pathological damage in dsGFP and dsU2AF injected mice. Data from each group are shown as means ± SEM. $^{**}p < 0.01$, $^{****}p < 0.0001$, t-test.

profiles during *S. japonicum* development. Our previous study showed that *S. japonicum* reaches sexual maturation in 2 weeks [25]. Our proteomic analysis successfully identified a total of 4666 proteins and 1714 DEPs from both genders and all time groups. The 37% coverage is reasonable because our study used only schistosomula and adults, specifically excluding eggs, miracidium, sporocysts, and cercariae.

Although various studies have benefited from integrative proteogenomic analysis [35,36], the relative mRNA quantity and protein level have a modest correlation [37]. Studies have shown that mRNA abundance only predicts protein abundance for approximately 40% of genes. The correlation coefficients between specific protein and mRNA levels vary across organisms, ranging from 0.09–0.46 in multi-cellular organisms [38]. In the current study 85.8% (4002/4666) of proteins were expressed; however, the dynamic change in profiles differed from profiles observed in the transcriptome study. Variations in the protein level can be attributed to differences in mRNA expression, as well as post-transcriptional and post-translational regulation, but not to measurement errors.

The majority of DEPs from 14–22 dpi displayed a predominant upregulation in male worms. Notably, 24 proteins, including ubiquitination, calcium-associated, and muscle contraction proteins, were upregulated in both sexes. The ubiquitin-proteasome system (UPS) is critical in the transition from cercariae-to-schistosomula and in *S. mansoni* egg production [39,40]. Calcium-associated proteins, which are upregulated following praziquantel treatment, have a pivotal role in the development of male and female worms [41]. From 22–26 dpi, the expression of upregulated proteins was notably greater in females compared to males, in agreement with the accelerated growth and development observed in females during this stage. This pattern identifies key proteins for potential strategies to inhibit schistosome fecundity. The specific upregulation of "translation" proteins and the downregulation of "signal transduction" proteins confirms the specialization of reproductive-related functions in female worms (S10 Fig). Moreover, a sole significantly enriched ribosome pathway

TABLE 1 | List of analyzed peptidases.

Gender	Peptidase	Annotation	14	18	22	26	Family
M	Sjp_0042800	CAAX prenyl protease 1 homolog					M48
M	Sjp_0041390	Puromycin-sensitive aminopeptidase-like isoform X2					M01
M	Sjp_0315740	Family S9 non-peptidase homologue (S09 family)					S09
M	Sjp_0217120	Lysosomal Pro-X carboxypeptidase precursor					S28
M	Sjp_0006800	Cathepsin D (lysosomal aspartyl protease)					A01
M	Sjp_0309370	Pre-sequence protease mitochondrial					M16
M	Sjp_0020240	Kyphoscoliosis peptidase					S15
M	Sjp_0025870	Aminopeptidase					M01
M	Sjp_0073580	Signal peptidase complex subunit 2 homolog					Unknown
M	Sjp_0080730	Prolyl endopeptidase					S09
M	Sjp_0218410	Cathepsin B-like peptidase (C01 family)					C01
M	Sjp_0300430	Family C2 unassigned peptidase (C02 family)					C02
M	Sjp_0007940	Cathepsin B endopeptidase					C01
M	Sjp_0048670	Zinc finger with UFM1-specific peptidase domain					C78
M	Sjp_0060580	Aspartyl aminopeptidase					M18
M	Sjp_0303030	Family S33 non-peptidase homologue (S33 family)					S33
F	Sjp_0205820	Family C12 unassigned peptidase (C12 family)					C12
F	Sjp_0042720	Kyphoscoliosis peptidase-like isoform X1					Unknown
F	Sjp_0009900	Putative methionyl aminopeptidase 2					M24
F	Sjp_0003450	26S protease regulatory subunit					M41
F	Sjp_0027540	Adam (A disintegrin and metalloprotease)					M12
F	Sjp_0097930	Methionyl aminopeptidase 1 (M24 family)					M24
F	Sjp_0204550	Leucyl aminopeptidase					M17

Blue: male-biased, Red: female-biased.

was identified (S4 Table), corroborating an earlier study that reported specialized ribosomal protein expression profiles upon male and female pairing [42].

Additionally, our research uncovered distinct sex-biased expression patterns of peptidases/proteases and receptors across various developmental stages (Table 1). Specifically, the CAAX isoprenyl protease I homolog, related to mating in *Saccharomyces*, and the lysosomal Pro-X carboxypeptidase precursor, demonstrate male-biased expression [43]. Greater than one-half of the 48 identified receptors exhibited sex-biased expression (S5 Table). The recent study also highlighted the importance of neuropeptides in schistosome gonad differentiation [44] and planarian germline development [45], suggesting that male and female schistosomes may utilize divergent peptidases and receptors to modulate the developmental processes, ranging from pairing-to-maturation.

Recent studies have advanced the hypothesis that U2AF serves as an essential gene associated with sex determination in schistosomes. These studies confirmed that W- and Z-U2AF possess different N-termini and have distinct male- and female-specific copies and expression, potentially representing a critical evolutionary step in determination of sex chromosomes and genotypes in schistosomes. It is suggested that W-U2AF might antagonize the activity of Z-U2AF to inhibit the splicing of one or more genes [46,47]. In our study we showed that Z-U2AF (Sjp_030142) protein was consistently upregulated in the 14-26 dpi of female worms. In addition, a more profound functional study was conducted for *Sj*U2AF. During *in vitro* culture, inhibition of Z-U2AF expression decreased worm viability and caused worm death. However, inhibition of W-U2AF expression did not significantly affect worm survival (data not shown). Given that we used dsRNA interference technology during the experiment, we could not completely invalidate the function of W-U2AF, leaving open the possibility that the residual W-U2AF might be operative. In addition, we only investigated U2AF function in schistosomula or adult worms, which cannot rule out a more significant role for W-U2AF in other developmental stages of *S. japonicum*. These areas require further investigation. The Z-U2AF study demonstrated that expression inhibition resulted in delayed growth, abnormal development of reproductive organs, and significant mortality of the worms *in vivo*. Our experiments also confirmed that Z-U2AF and W-U2AF exhibit distinct functional characteristics, but specific functions require more detailed investigation.

In conclusion, our results highlight distinct patterns of DEPs between male and female worms throughout schistosome development. The dynamic expression profile of protein provides new insight into cell function and interactions between the sexes during schistosome maturation *in vivo*. Among the genes examined, U2AF was identified as indispensable for the growth and development of reproductive organs in *S. japonicum*, as well as being necessary for maintaining worm parasitism within the host. Future studies based on these results will undoubtedly continue to reveal further biological insight into schistosome development and anti-schistosome therapeutics.

ACKNOWLEDGEMENTS

This work was supported by funding from the National Natural Science Foundation of China (grant no. 31972699), the Shanghai Municipal Science and Technology Committee of Shanghai Outstanding Academic Leaders Plan (grant no. 18XD1400400), the Natural Science Foundation of Anhui Province (grant no. 2008085QH430), and the Science and Technology Leading Talent Team plan (grant no. 2022SLJRC0023).

CONFLICTS OF INTEREST

The authors declare that they have no competing interests.

REFERENCES

1. Barnett R. Schistosomiasis. Lancet. 2018;392(10163):2431.
2. Hotez PJ, Fenwick A. Schistosomiasis in Africa: an emerging tragedy in our new global health decade. PLoS Negl Trop Dis. 2009;3(9):e485.
3. Gray DJ, McManus DP, Li Y, Williams GM, Bergquist R, Ross AG. Schistosomiasis elimination: lessons from the past guide the future. Lancet Infect Dis. 2010;10(10):733-736.
4. Utzinger J, Raso G, Brooker S, De Savigny D, Tanner M, ØRnbjerg N, et al. Schistosomiasis and neglected tropical diseases: towards integrated and sustainable control and a word of caution. Parasitology. 2009;136(13):1859-1874.
5. Nelwan ML. Schistosomiasis: life cycle, diagnosis, and control. Curr Ther Res. 2019;91:5-9.
6. Nation CS, Da'dara AA, Marchant JK, Skelly PJ. Schistosome migration in the definitive host. PLoS Negl Trop Dis. 2020;14(4):e0007951.
7. LoVerde PT. Presidential address. Sex and schistosomes: an interesting biological interplay with control implications. J Parasitol. 2002;88(1):3-13.
8. Costain AH, MacDonald AS, Smits HH. Schistosome egg migration: mechanisms, pathogenesis and host immune responses. Front Immunol. 2018;9:3042.
9. Mathieson W, Wilson RA. A comparative proteomic study of the undeveloped and developed Schistosoma mansoni egg and its contents: the miracidium, hatch fluid and secretions. Int J Parasitol. 2010;40(5):617-628.
10. Wang T, Zhao M, Rotgans BA, Strong A, Liang D, Ni G, et al. Proteomic analysis of the schistosoma mansoni miracidium. PLoS One. 2016;11(1):e0147247.
11. Knudsen GM, Medzihradszky KF, Lim KC, Hansell E, McKerrow JH. Proteomic analysis of Schistosoma mansoni cercarial secretions. Mol Cell Proteomics. 2005;4(12):1862-1875.
12. Liu M, Ju C, Du XF, Shen HM, Wang JP, Li J, et al. Proteomic analysis on cercariae and schistosomula in reference to potential proteases involved in host invasion of schistosoma japonicum larvae. J Proteome Res. 2015;14(11):4623-4634.
13. Sotillo J, Pearson M, Potriquet J, Becker L, Pickering D, Mulvenna J, et al. Extracellular vesicles secreted by Schistosoma mansoni contain protein vaccine candidates. Int J Parasitol. 2016;46(1):1-5.
14. Cao X, Fu Z, Zhang M, Han Y, Han Q, Lu K, et al. Excretory/secretory proteome of 14-day schistosomula, Schistosoma japonicum. J Proteomics. 2016;130:221-230.
15. Cao X, Fu Z, Zhang M, Han Y, Han H, Han Q, et al. iTRAQ-based comparative proteomic analysis of excretory-secretory proteins of schistosomula and adult worms of Schistosoma japonicum. J Proteomics. 2016;138:30-39.

16. Hong Y, Sun A, Zhang M, Gao F, Han Y, Fu Z, et al. Proteomics analysis of differentially expressed proteins in schistosomula and adult worms of Schistosoma japonicum. Acta Trop. 2013;126(1):1-10.
17. Cheng GF, Lin JJ, Feng XG, Fu ZQ, Jin YM, Yuan CX, et al. Proteomic analysis of differentially expressed proteins between the male and female worm of Schistosoma japonicum after pairing. Proteomics. 2005;5(2):511-521.
18. Wisniewski JR, Zougman A, Nagaraj N, Mann M. Universal sample preparation method for proteome analysis. Nat Methods. 2009;6(5):359-362.
19. Wang J, Paz C, Padalino G, Coghlan A, Lu Z, Gradinaru I, et al. Large-scale RNAi screening uncovers therapeutic targets in the parasite Schistosoma mansoni. Science. 2020;369(6511):1649-1653.
20. Wang J, Chen R, Collins JJ 3rd. Systematically improved in vitro culture conditions reveal new insights into the reproductive biology of the human parasite Schistosoma mansoni. PLoS Biol. 2019;17(5):e3000254.
21. Li J, Xiang M, Zhang R, Xu B, Hu W. RNA interference in vivo in Schistosoma japonicum: establishing and optimization of RNAi mediated suppression of gene expression by long dsRNA in the intra-mammalian life stages of worms. Biochem Biophys Res Commun. 2018;503(2):1004-1010.
22. Fitzpatrick JM, Hoffmann KF. Dioecious Schistosoma mansoni express divergent gene repertoires regulated by pairing. Int J Parasitol. 2006;36(10-11):1081-1089.
23. Sun J, Wang SW, Li C, Hu W, Ren YJ, Wang JQ. Transcriptome profilings of female Schistosoma japonicum reveal significant differential expression of genes after pairing. Parasitol Res. 2014;113(3):881-892.
24. Loeffler IK, Bennett JL. A rab-related GTP-binding protein in Schistosoma mansoni. Mol Biochem Parasitol. 1996;77(1):31-40.
25. Wang J, Yu Y, Shen H, Qing T, Zheng Y, Li Q, et al. Dynamic transcriptomes identify biogenic amines and insect-like hormonal regulation for mediating reproduction in Schistosoma japonicum. Nat Commun. 2017;8:14693.
26. Liu F, Lu J, Hu W, Wang SY, Cui SJ, Chi M, et al. New perspectives on host-parasite interplay by comparative transcriptomic and proteomic analyses of Schistosoma japonicum. PLoS Pathog. 2006;2(4):e29.
27. Braschi S, Wilson RA. Proteins exposed at the adult schistosome surface revealed by biotinylation. Mol Cell Proteomics. 2006;5(2):347-356.
28. van Balkom BW, van Gestel RA, Brouwers JF, Krijgsveld J, Tielens AG, Heck AJ, et al. Mass spectrometric analysis of the Schistosoma mansoni tegumental sub-proteome. J Proteome Res. 2005;4(3):958-966.
29. Liu F, Hu W, Cui SJ, Chi M, Fang CY, Wang ZQ, et al. Insight into the host-parasite interplay by proteomic study of host proteins copurified with the human parasite, Schistosoma japonicum. Proteomics. 2007;7(3):450-462.
30. Curwen RS, Ashton PD, Johnston DA, Wilson RA. The Schistosoma mansoni soluble proteome: a comparison across four life-cycle stages. Mol Biochem Parasitol. 2004;138(1):57-66.
31. Liu F, Cui SJ, Hu W, Feng Z, Wang ZQ, Han ZG. Excretory/secretory proteome of the adult developmental stage of human blood fluke, Schistosoma japonicum. Mol Cell Proteomics. 2009;8(6):1236-1251.
32. Jang-Lee J, Curwen RS, Ashton PD, Tissot B, Mathieson W, Panico M, et al. Glycomics analysis of Schistosoma mansoni egg and cercarial secretions. Mol Cell Proteomics. 2007;6(9):1485-1499.
33. Hong Y, Cao X, Han Q, Yuan C, Zhang M, Han Y, et al. Proteome-wide analysis of lysine acetylation in adult Schistosoma japonicum worm. J Proteomics. 2016;148:202-212.
34. Cheng G, Luo R, Hu C, Lin J, Bai Z, Zhang B, et al. TiO_2-based phosphoproteomic analysis of schistosomes: characterization of phosphorylated proteins in the different stages and sex of Schistosoma japonicum. J Proteome Res. 2013;12(2):729-742.
35. Stavrianakou M, Perez R, Wu C, Sachs MS, Aramayo R. Draft de novo transcriptome assembly and proteome characterization of the electric lobe of Tetronarce californica: a molecular tool for the study of cholinergic neurotransmission in the electric organ. BMC Genomics. 2017;18(1):611.
36. Mok L, Wynne JW, Tachedjian M, Shiell B, Ford K, Matthews DA, et al. Proteomics informed by transcriptomics for characterising differential cellular susceptibility to Nelson Bay orthoreovirus infection. BMC Genomics. 2017;18(1):615.
37. Gygi SP, Rochon Y, Franza BR, Aebersold R. Correlation between protein and mRNA abundance in yeast. Mol Cell Biol. 1999;19(3):1720-1730.
38. de Sousa Abreu R, Penalva LO, Marcotte EM, Vogel C. Global signatures of protein and mRNA expression levels. Mol Biosyst. 2009;5(12):1512-1526.
39. Guerra-Sa R, Castro-Borges W, Evangelista EA, Kettelhut IC, Rodrigues V. Schistosoma mansoni: functional proteasomes are required for development in the vertebrate host. Exp Parasitol. 2005;109(4):228-236.
40. Mathieson W, Castro-Borges W, Wilson RA. The proteasome-ubiquitin pathway in the Schistosoma mansoni egg has development- and morphology-specific characteristics. Mol Biochem Parasitol. 2011;175(2):118-125.
41. You H, McManus DP, Hu W, Smout MJ, Brindley PJ, Gobert GN. Transcriptional responses of in vivo praziquantel exposure in schistosomes identifies a functional role for calcium signalling pathway member CamKII. PLoS Pathog. 2013;9(3):e1003254.
42. Sun J, Li C, Wang S. The up-regulation of ribosomal proteins further regulates protein expression profile in female schistosoma japonicum after pairing. PLoS One. 2015;10(6):e0129626.
43. Schistosoma japonicum Genome Sequencing and Functional Analysis Consortium. The Schistosoma japonicum genome reveals features of host-parasite interplay. Nature. 2009;460(7253):345-351.
44. Lu Z, Sessler F, Holroyd N, Hahnel S, Quack T, Berriman M, et al. Schistosome sex matters: a deep view into gonad-specific and pairing-dependent transcriptomes reveals a complex gender interplay. Sci Rep. 2016;6:31150.
45. Collins JJ 3rd, Hou X, Romanova EV, Lambrus BG, Miller CM, Saberi A, et al. Genome-wide analyses reveal a role for peptide hormones in planarian germline development. PLoS Biol. 2010;8(10):e1000509.
46. Elkrewi M, Moldovan MA, Picard MAL, Vicoso B. Schistosome W-linked genes inform temporal dynamics of sex chromosome evolution and suggest candidate for sex determination. Mol Biol Evol. 2021;38(12):5345-5358.
47. Buddenborg SK, Tracey A, Berger DJ, Lu Z, Doyle SR, Fu B, et al. Assembled chromosomes of the blood fluke Schistosoma mansoni provide insight into the evolution of its ZW sex-determination system. bioRxiv. 2021:2021.2008. 2013.456314.